Max-Planck-Institut für Mathematik in den Naturwissenschaften Leipzig

Grid-based lattice summation of electrostatic potentials by low-rank tensor approximation

(revised version: January 2014)

by

Venera Khoromskaia and Boris N. Khoromskij

Preprint no.: 116 2013

Grid-based lattice summation of electrostatic potentials by low-rank tensor approximation

V. KHOROMSKAIA* B. N. KHOROMSKIJ**

January 17, 2014

Abstract

We introduce and study the grid-based rank-structured tensor method for fast and accurate calculation of the lattice sums of Coulomb interactions on large 3D periodic-structured compounds. The approach is based on the low-rank canonical tensor representation of the Newton kernels discretized in a computational box using fine $N \times N \times N$ 3D Cartesian grid. This reduces the 3D summation to a sequence of tensor operations involving only 1D vector sums, where each N-vector represents the canonical component in the tensor approximation to the lattice-translated Newton kernel. In the case of a supercell consisting of $L \times L \times L$ unit cells in a box the numerical cost scales linearly in the grid-size, n as $O(NL)$. For periodic boundary conditions, the storage demand remains proportional to the size of a unit cell, N/L, while the numerical cost reduces to $O(N)$, that outperforms the FFT-based Ewald summation approaches of the complexity $O(N^3 \log N)$. The complexity scaling in the grid parameter n can be reduced even to the logarithmic scale $O(\log N)$ by the quantics tensor approximation method. We prove an upper bound of the quantics rank for the canonical vectors in the lattice sum. This opens the way to numerical simulations including large lattice sums in a supercell (i.e. as $L \to \infty$) and their multiple replicas in periodic setting. This approach is beneficial in applications which require further functional calculus with the lattice potential, say, scalar product with a function, integration or differentiation, which can be performed easily in tensor arithmetics on large 3D grids with 1D cost. Numerical tests illustrate the performance of the tensor summation method and confirm the estimated bounds on the quantics rank.

AMS Subject Classification: 65F30, 65F50, 65N35, 65F10
Key words: Lattice sums, periodic systems, Ewald summation, tensor numerical methods, canonical tensor decomposition, quantics tensor approximation, Hartree-Fock equation, Coulomb potential, molecular dynamics.

*Max-Planck-Institute for Mathematics in the Sciences, Inselstr. 22-26, D-04103 Leipzig, Germany (vekh@mis.mpg.de).

**Max-Planck-Institute for Mathematics in the Sciences, Inselstr. 22-26, D-04103 Leipzig, Germany (bokh@mis.mpg.de).

1 Introduction

There are several challenges in the numerical treatment of periodic systems and perturbed periodic systems in quantum chemical computations for crystalline, metallic and polymer-type compounds, see [12, 43, 36, 47] and [46, 40, 37, 6, 38]. One of them is the the lattice summation over a huge number of Newton kernels distributed on large 3D computational grid. This problem is also considered to be a demanding computational task in the numerical treatment of long-range electrostatic interactions in molecular dynamics simulations of large solvated biological systems [44, 20, 8]. In these applications the efficient calculation of quantities like potential energy function or interparticle forces remains to be of main interest.

Tracing back to Ewald summation techniques [13], the development of lattice-sum methods in numerical simulation of particle interactions in large molecular systems has led to established algorithms for evaluating long-range electrostatic potentials of multiparticle systems, see for example [7, 44, 20, 8, 39] and references therein. These methods usually combine the original Ewald summation approach with the Fast Fourier Transform (FFT) or fast multipole methods [16]. The Ewald summation techniques were shown to be particularly attractive for computation of a potential energy and forces of many-particle systems with long-range interaction potential in periodic boundary conditions.

In this paper, we introduce the new approach to this complicated numerical problem based on the idea of low-rank tensor decomposition applied to the overall lattice sum of Newton kernels discretized on large Cartesian grid. This approach was initiated by the numerical observations in [31, 23] that the Tucker rank of the 3D lattice sum of Slater functions remains uniformly bounded in the number of cells.

As the important ingredient, we apply tensor numerical methods now recognized as the a powerful tool for solution of multidimensional partial differential equations (PDEs) discretized by traditional grid-based schemes. Beginning from the DMRG-based matrix product states decomposition in quantum physics and chemistry [48, 45] and then tensor techniques in multilinear algebra (see the literature surveys [35, 30, 17, 15] and further details in Appendix), they were recently developed to the new branch of numerical analysis, tensor numerical methods, providing algorithms for solving multidimensional PDEs with linear complexity scaling in the dimension [29]. One of the first steps in development of the tensor numerical methods was the 3D grid-based tensor-structured solution of the Hartree-Fock equation in electronic structure calculations based on the efficient algorithms for calculation of the 3D convolution integral operators in 1D complexity [27, 33, 23, 24].

Compared with the traditional Ewald summation techniques applied merely to the point-values of the potentials, our tensor method provides the adaptive global decomposition of a sum of interacting potentials in the completely algebraic way, so that the resultant sum is computed simultaneously on the fine 3D Cartesian grid in the whole computational box (supercell) or in the unit cell (periodic setting).

The grid-based tensor approach is beneficial in applications requiring further functional calculus with the lattice potential sum, for example, interpolation, scalar product with a function, integration or differentiation (computation of energies or forces), which can be performed on large 3D grids using tensor arithmetics of sub-linear cost [23, 32]. The latter advantage makes the tensor method promising in electronic structure calculations for computation of the Galerkin projections of the nuclear potential onto the physically relevant

reduced basis sets like atomic or molecular orbitals.

Advantages of rank-structured tensor approach applied to the lattice summation problem are achieved due to combination of two basic ideas: on the one hand, we exploit the global nearly tensor-product geometric structure in the 3D location of interacting "particles" and, on the other hand, we apply the efficient local-global separable tensor decomposition (in canonical format) to the shifted Newton kernels represented on the fine $N \times N \times N$ spacial grid which discretizes the uniformly distributed $L \times L \times L$ lattice structure in a supercell. The latter observation allows us to prove that the separation rank of the total sum on a supercell does not exceed the rank of the canonical tensor representing the single Newton kernel. As a result, we reduce the 3D summation to the sequence of 1D sums operating with L skeleton vectors each of size N, where the univariate grid-size N is linearly proportional to L, $N = nL$.

In the case of a supercell in a box the storage size is then bounded by $O(L)$, while the summation cost is estimated by $O(NL)$. The latter can be reduced to $O(L \log N)$ by using the quantized approximation (QTT method) of long canonical vectors. Notice that a sum over supercell in a box cannot be treated by the FFT method. In turn, the fast multipole method scales linear-logarithmic in the volume size, $L^3 \log L$.

In periodic boundary conditions, the respective 1D sums operate only with short vectors of size $n = N/L$, where n denotes here the number of grid points per unit cell. The storage and computational costs are estimated by $O(n)$ and $O(Ln)$, respectively. In turn, in this case the FFT based approach scales at least cubically in L, $O(L^3 \log L)$. Due to the low cost of tensor method in the limit of large lattice size L, the conditionally convergent sums in periodic setting can be regularized by subtraction of the constant term which can be evaluated numerically by the Richardson extrapolation on a sequence of lattice parameters $L, 2L, 4L$ etc. (see §3.2). Hence, in the new framework the analytic treatment is not required.

It is worth to note that the presented tensor method is applicable to the lattice sums of rather general interaction potentials which allow the efficient local-plus-separable approximation. In particular, it can be applied to a wide class of commonly used interaction potentials, for example, to the Coulomb, Slater, Yukawa, Stokeslet, Lennard-Jones or van der Waals interactions. In all these cases the existence of low-rank grid-based tensor decomposition can be proved and it can be implemented numerically by analytic-algebraic methods as in the case of the Newton kernel. This tensor approach can be easily extended to slightly perturbed periodic systems, for example, to the case of vacancies in the spacial distribution of electrostatic potentials, a small perturbation in positions of electron charges and other defects. In this case the combination with fast multipole method [16] seems promising.

The reminder of the paper is structured as follows. Section 2 introduces the low-rank approximation to the single Newton kernel represented on a $N \times N \times N$ tensor grid in a supercell. Section 3 describes the main results on tensor decomposition of the lattice sum in a box as well as in the periodic setting. The storage estimates and complexity analysis are provided. In Section 4, we prove the low QTT-rank approximation of the canonical vectors in the lattice sum of the Newton kernels that justifies the logarithmic complexity scaling of the tensor summation scheme. The discussion in Section 5 concludes the paper. For the readers convenience, Appendix outlines the main notions in multilinear tensor algebra to be used in the paper.

2 Tensor decomposition of the Coulomb interaction

2.1 Grid-based canonical representation of the Newton kernel

Methods of separable approximation to the 3D Newton kernel using the Gaussian sums have been addressed in the chemical and mathematical literature since [3] and [4, 5], respectively.

In this section, we briefly recall the grid-based method for the low-rank tensor representation of the 3D Newton kernel $\frac{1}{\|x\|}$ by its projection onto the set of piecewise constant basis functions, see [27] for more details. Based on the results in [14, 18, 1], this approximation can be proven to converge almost exponentially in the rank parameter. For the readers convenience, we now recall the main ingredients of this tensor approximation scheme [1].

In the computational domain $\Omega = [-b/2, b/2]^3$, let us introduce the uniform $n \times n \times n$ rectangular Cartesian grid Ω_n with the mesh size $h = b/n$. Let $\{\psi_{\mathbf{i}}\}$ be the set of tensor-product piecewise constant basis functions, $\psi_{\mathbf{i}}(\mathbf{x}) = \prod_{\ell=1}^{d} \psi_{i_\ell}^{(\ell)}(x_\ell)$ for $\mathbf{i} = (i_1, i_2, i_3) \in \mathcal{I} := I \times I \times I$, $i_\ell \in I = \{1, ..., n\}$. The Newton kernel can be discretized by the projection/collocation method in the form of a third order tensor of size $n \times n \times n$,

$$\mathbf{P} := [p_{\mathbf{i}}]_{\mathbf{i}\in\mathcal{I}} \in \mathbb{R}^{n\times n\times n}, \quad p_{\mathbf{i}} = \int_{\Omega_{\mathbf{i}}} \frac{\psi_{\mathbf{i}}(\mathbf{x})}{\|\mathbf{x}\|}\, \mathrm{d}\mathbf{x}, \quad \text{where} \quad \Omega_{\mathbf{i}} = \mathrm{supp}(\psi_{\mathbf{i}}). \tag{2.1}$$

The low-rank canonical decomposition of $\mathbf{P}$ is based on using exponentially convergent sinc-quadratures for approximation of its Laplace-Gauss transform,

$$\frac{1}{\|\mathbf{x}\|} = \frac{1}{\sqrt{\pi}} \int_{\mathbb{R}} e^{-t^2\|\mathbf{x}\|^2}\, \mathrm{d}t = \frac{1}{\sqrt{\pi}} \int_{\mathbb{R}} \prod_{\ell=1}^{3} e^{-t^2 (x_\ell)^2}\, \mathrm{d}t, \quad \|\mathbf{x}\| > 0. \tag{2.2}$$

Plugging (2.2) in (2.1), we arrive at the entrywise representation of the tensor $\mathbf{P}$,

$$p_{\mathbf{i}} = \frac{1}{\sqrt{\pi}} \int_{\mathbb{R}} \int_{\Omega} \psi_{\mathbf{i}}(\mathbf{x}) e^{-\|\mathbf{x}\|^2 t^2}\, \mathrm{d}\mathbf{x}\, \mathrm{d}t = \int_{\mathbb{R}} \prod_{\ell=1}^{3} \mathbf{B}_{i_\ell}^{(\ell)}(t)\, \mathrm{d}t, \tag{2.3}$$

with

$$\mathbf{B}_{i_\ell}^{(\ell)}(t) = \pi^{-1/6} \int_{\Omega_\ell} \psi_{i_\ell}^{(\ell)}(x_\ell) e^{-x_\ell^2 t^2} \mathrm{d}x_\ell,$$

which remains valid for $\|\mathbf{x}\| > 0$, i.e. for all entries satisfying $dist(\mathrm{supp}(\psi_{\mathbf{i}}), 0) > 0$. Furthermore, since in the integral (2.3) the spatial variables are separated, the tensor $\mathbf{P}$ obeys the integral representation via a family of rank-1 tensors,

$$\mathbf{P} = \int_{\mathbb{R}} \bigotimes_{\ell=1}^{3} \mathbf{B}^{(\ell)}(t)\, \mathrm{d}t \quad \text{with} \quad \mathbf{B}^{(\ell)}(t) = \{\mathbf{B}_{i_\ell}^{(\ell)}(t)\} \in \mathbb{R}^{n_\ell}. \tag{2.4}$$

Construction of an accurate quadrature to approximate (2.4) for all elements $p_{\mathbf{i}}$ ($\mathbf{i} \in \mathcal{I}$) simultaneously, and with possibly small number of terms solves the problem.

For the given precision $\varepsilon > 0$, we apply the asymptotically optimal sinc-quadrature formula on $\mathbb{R}$ to the integral (2.4) of a tensor-valued function, to obtain the rank-R ($R = 2M+1$)

canonical representation

$$\mathbf{P} \approx \mathbf{P}_R = \sum_{k=-M}^{M} g_k \bigotimes_{\ell=1}^{3} \mathbf{B}^{(\ell)}(t_k), \quad g_k,\, t_k \in \mathbb{R},$$

where $R = 2M + 1$ and M is chosen in such a way that in the max-norm

$$\|\mathbf{P} - \mathbf{P}_R\| \le \varepsilon \|\mathbf{P}\|.$$

Proposition 2.1 *([18, 1]) The choice for the quadrature parameters (applicable for* $0 < \|\mathbf{x}\|$*)*

$$t_k = k\mathfrak{h}_M,\ g_k = \mathfrak{h}_M,\ \mathfrak{h}_M = C_0 \log(M)/M,\ C_0 \in \mathbb{R}_+, \tag{2.5}$$

leads to the exponential convergence in M*,*

$$\|\mathbf{P} - \mathbf{P}_R\| \le C\, e^{-\beta\sqrt{M}} \|\mathbf{P}\| \quad \textit{with}\ \ C, \beta \in \mathbb{R}_+.$$

The symmetry of quadrature points implies the tensor-rank estimate $R \le M + 1$*.*

In the case of a bounded interval $0 < \|\mathbf{x}\| \le A = O(b) < \infty$, an improved convergence rate for the quadrature can be achieved by using the transformation of variables $t = \sinh(u)$,

$$\mathbf{P} = \int_{\mathbb{R}} \cosh(u) \bigotimes_{\ell=1}^{d} \mathbf{B}^{(\ell)}(\sinh(u))\, \mathrm{d}u \approx \sum_{k=0}^{M} g_k \bigotimes_{\ell=1}^{d} \mathbf{B}^{(\ell)}(t_k) := \mathbf{P}_R. \tag{2.6}$$

If quadrature points and weights in (2.6) are chosen as

$$t_k = \sinh(k\mathfrak{h}_M), \quad g_k = \begin{cases} \mathfrak{h}_M & \text{for } k = 0 \\ 2\,\mathfrak{h}_M \cosh(k\mathfrak{h}_M) & \text{for } 0 < k < M, \end{cases} \tag{2.7}$$

with $\mathfrak{h}_M$ as in (2.5), then the quadrature (2.6) - (2.7) converges in M asymptotically as

$$\|\mathbf{P} - \mathbf{P}_R\| \le C\, e^{-\beta M/((1+\log A)\log M)} \|\mathbf{P}\| \quad \text{with}\ \ C, \beta \in \mathbb{R}_+.$$

Now we define the rank-R canonical tensor[1]

$$\mathbf{P}_R = \sum_{q=1}^{R} P_q^{(1)} \otimes P_q^{(2)} \otimes P_q^{(3)} \in \mathbb{R}^{n\times n\times n}, \tag{2.8}$$

approximating the 3D Newton kernel $\frac{1}{\|x\|}$ $(x \in \Omega)$, centered at the origin, with $R \le M + 1$.

Table 2.1 shows times for generating a canonical rank-R tensor approximation of the Newton kernel over $n \times n \times n$ 3D Cartesian grid. Note that our algorithms are implemented in Matlab, and the times are shown for a terminal of the 8 AMD Opteron Dual-Core processor. We observe a logarithmic scaling of the canonical rank R in the grid size. The compression rate denotes the ratio $n^3/(nR)$.

Notice that the low-rank canonical decomposition of the tensor $\mathbf{P}$ is the problem independent task, hence the respective canonical vectors can be precomputed at once on very large 3D $n \times n \times n$ grid, and then stored for the multiple use. The storage size is bounded by $O(Rn)$.

The main idea of the tensor lattice summation method to be described in the following is based on the use of low-rank canonical representation to the single Newton kernel $\mathbf{P}_R$ in the bounding box, translated and restricted onto the 3D product grid that specifies the lattice.

[1]The notion "rank-R canonical tensor" in our presentation does not mean that R is the minimal canonical rank of the target tensor, but it just denotes the actual number of terms in the canonical sum. The possible rank reduction is not significant in the discussion of our algorithms.

grid size n^3	8192^3	16384^3	32768^3	65536^3	131072^3
Time (sec.)	6	16	61	241	1000
Canonical rank R	34	37	39	41	43
Compression rate	$2 \cdot 10^6$	$7 \cdot 10^6$	$2 \cdot 10^7$	$1 \cdot 10^8$	$4 \cdot 10^8$

Table 2.1: CPU times (Matlab code) to compute $\mathbf{P}_R$ for the Newton kernel in a box.

2.2 Tensor summation of the Coulomb interactions in a unit cell

As the basic example in electronic structure calculations, we consider the nuclear (core) potential operator describing the Coulomb interaction of electrons with the nuclei, defined by the function $v_c(x)$ in the scaled unit cell $\Omega = [-b/2, b/2]^3$,

$$v_c(x) = \sum_{\nu=1}^{M_0} \frac{Z_\nu}{\|x - a_\nu\|}, \quad Z_\nu > 0, \;\; x, a_\nu \in \Omega \subset \mathbb{R}^3, \tag{2.9}$$

where M_0 is the number of nuclei in Ω, and a_ν, Z_ν, represent their coordinates and charges, respectively.

We begin with approximating the non-shifted 3D Newton kernel $\frac{1}{\|x\|}$ on the auxiliary extended box $\widetilde{\Omega} = [-b, b]^3$, by its projection onto the basis set $\{\psi_{\mathbf{i}}\}$ of piecewise constant functions defined on the uniform $2n \times 2n \times 2n$ tensor grid Ω_{2n} with the mesh size h, as described in Section 2.1. This defines the "master" rank-R canonical tensor as above

$$\widetilde{\mathbf{P}}_R = \sum_{q=1}^{R} P_q^{(1)} \otimes P_q^{(2)} \otimes P_q^{(3)} \in \mathbb{R}^{2n \times 2n \times 2n}. \tag{2.10}$$

Let us denote by $P^{(\ell)} = [P_1^{(\ell)}, ..., P_R^{(\ell)}] \in \mathbb{R}^{2n \times R}$, $(\ell = 1, 2, 3)$ the related factor matrices of the canonical tensor $\widetilde{\mathbf{P}}_R$ in (2.10).

For ease of exposition, we assume that each nuclear coordinate a_ν is located exactly at a grid-point $a_\nu = (i_\nu h - b/2, j_\nu h - b/2, k_\nu h - b/2)$, with some $1 \le i_\nu, j_\nu, k_\nu \le n$. Now we are able to introduce the rank-1 windowing operator $\mathcal{W}_\nu = \mathcal{W}_\nu^{(1)} \otimes \mathcal{W}_\nu^{(2)} \otimes \mathcal{W}_\nu^{(3)}$ for $\nu = 1, ..., M_0$ by

$$\mathcal{W}_\nu \widetilde{\mathbf{P}}_R := \widetilde{\mathbf{P}}_R(i_\nu + n/2 : i_\nu + 3/2n; j_\nu + n/2 : j_\nu + 3/2n; k_\nu + n/2 : k_\nu + 3/2n) \in \mathbb{R}^{n \times n \times n}, \tag{2.11}$$

With this notation, the total electrostatic potentials $v_c(x)$ in the computational box Ω is approximately represented by a canonical tensor sum

$$\begin{aligned} \mathbf{P}_c &= \sum_{\nu=1}^{M_0} Z_\nu \mathcal{W}_\nu \widetilde{\mathbf{P}}_R \\ &= \sum_{\nu=1}^{M_0} Z_\nu \sum_{q=1}^{R} \mathcal{W}_\nu^{(1)} P_q^{(1)} \otimes \mathcal{W}_\nu^{(2)} P_q^{(2)} \otimes \mathcal{W}_\nu^{(3)} P_q^{(3)} \in \mathbb{R}^{n \times n \times n}, \end{aligned}$$

with the rank bound

$$rank(\mathbf{P}_c) \le M_0 R,$$

where every rank-R canonical tensor $\mathcal{W}_\nu \widetilde{\mathbf{P}}_R \in \mathbb{R}^{n\times n\times n}$ is thought as a sub-tensor of the master tensor $\widetilde{\mathbf{P}}_R \in \mathbb{R}^{2n\times 2n\times 2n}$ obtained by its shifting and restriction (windowing) onto the $n\times n\times n$ grid in the unit cell Ω, $\Omega_n \subset \Omega_{2n}$. Here a shift from the origin is specified according to the coordinates of the corresponding nuclei, a_ν, counted in the h-units.

For example, the electrostatic potential centered at the origin, i.e. with $a_\nu = 0$, corresponds to the restriction of $\widetilde{\mathbf{P}}_R$ onto the initial computational box Ω_n, i.e. to the index set (assume that n is even)

$$\{[n/2+i]\times[n/2+j]\times[n/2+k]\},\quad i,j,k\in\{1,...,n\}.$$

Remark 2.2 *The rank estimate (2.12) for the sum of electrostatic potentials in a unit cell, $R_c = rank(\mathbf{P}_c) \le M_0 R$, is usually too pessimistic. Our numerical tests for moderate size molecules indicate that the rank of the (M_0R)-term canonical sum in (2.12) can be reduced merely to the same value R as for the master tensor in (2.10). This rank optimization can be implemented by the multigrid version of the canonical rank reduction algorithm, canonical-Tucker-canonical [32]. The resultant canonical tensor will be denoted by $\widehat{\mathbf{P}}_c$.*

The following example illustrates an application of the proposed grid-based tensor representation to calculation of the Galerkin projection of the exact sum $v_c(x)$ onto a certain well separable basis set in 3D. For example, it might be the GTO-type atomic orbital basis often used in quantum chemical computations.

Example 2.3 *Given the set of continuous basis functions, $\{g_\mu(x)\}$, $(\mu = 1,...,N_b)$, then each of them can be discretized by a third order tensor, $\mathbf{G}_\mu = [g_\mu(x_1(i),x_2(j),x_3(k))]_{i,j,k=1}^n \in \mathbb{R}^{n\times n\times n}$, obtained by sampling of $g_\mu(x)$ at the midpoints $(x_1(i),x_2(j),x_3(k))$ of the grid-cells indexed by (i,j,k). Suppose, without loss of generality, that it is a rank-1 tensor, $rank(\mathbf{G}_\mu) = 1$, i.e. it has a separable form*

$$\mathbf{G}_\mu = G_\mu^{(1)} \otimes G_\mu^{(2)} \otimes G_\mu^{(3)} \in \mathbb{R}^{n\times n\times n},$$

with the skeleton vectors $G_\mu^{(\ell)} \in \mathbb{R}^n$, associated with mode $\ell = 1,2,3$. Now, each entry of the Galerkin matrix, $V_c = \{v_{km}\} \in \mathbb{R}^{N_b\times N_b}$, representing the potential sum $v_c(x)$ in (2.9), is calculated (approximated) by the simple tensor operation

$$v_{km} = \int_{\mathbb{R}^3} v_c(x) g_k(x) g_m(x) dx \approx \langle \mathbf{G}_k \odot \mathbf{G}_m, \mathbf{P}_c\rangle,\quad 1\le k,m\le N_b, \tag{2.12}$$

where $\odot$ means Hadamard (entrywise) product of tensors.

This scheme also applies to the lattice sum in a supercell to be discussed in the following.

To conclude this section, we notice that the approximation error $\varepsilon > 0$ caused by a separable representation of the nuclear potential is controlled by the rank parameter $R_c = rank(\mathbf{P}_c) \approx C\,R$, where C does depend on M_0. Now letting $rank(\mathbf{G}_m) = 1$ implies that each matrix element is to be computed with linear complexity in n, $O(R\,n)$. The exponential convergence of the canonical approximation in the rank parameter R allows us the optimal choice $R = O(|\log\varepsilon|)$ adjusting the overall complexity bound $O(|\log\varepsilon|\,n)$, independent on M_0.

3 Fast lattice summation using canonical tensors

3.1 3D lattice-sum method by tensor decomposition in a box

In this section, we discuss an extended system in a box. Given the potential sum v_c in the unit reference cell $\Omega = [-b/2, b/2]^d$, $d = 3$, of size $b \times b \times b$, we consider an interaction potential in a supercell

$$\Omega_L = B_1 \times B_2 \times B_3,$$

consisting of a union of $L_1 \times L_2 \times L_3$ unit cells $\Omega_{\mathbf{k}}$, obtained from Ω by a shift proportional to b in each variable, and specified by the lattice vector $b\mathbf{k}$, $\mathbf{k} = (k_1, k_2, k_3) \in \mathbb{Z}^d$, $0 \le k_\ell \le L_\ell - 1$, $(\ell = 1, 2, 3)$. Here $B_\ell = [-b/2, b/2 + (L_\ell - 1)b]$ for $L_\ell \in \mathbb{N}$, where $L_\ell = 1$ corresponds to one-layer systems in the respective variable. Recall that we have $b = nh$, where h is the grid size that is the same for all spacial variables. Notice that in periodic setting the symmetric supercell corresponding to the indexing $-L_\ell \le k_\ell \le L_\ell$ is the commonly used notation.

In the case of extended system in a box, further called case (B), the summation problem for the total potential v_{c_L} is formulated in the box $\Omega_L = \bigcup_{k_1,k_2,k_3=1}^{L} \Omega_{\mathbf{k}}$. On each $\Omega_{\mathbf{k}} \subset \Omega_L$, the potential sum of interest, $v_{\mathbf{k}}(x) = (v_{c_L})_{|\Omega_{\mathbf{k}}}$, is obtained by summation over all unit cells in Ω_L,

$$v_{\mathbf{k}}(x) = \sum_{\nu=1}^{M_0} \sum_{k_1,k_2,k_3=0}^{L-1} \frac{Z_\nu}{\|x - a_\nu(k_1, k_2, k_3)\|}, \quad x \in \Omega_{\mathbf{k}}, \tag{3.1}$$

where $a_\nu(k_1, k_2, k_3) = a_\nu + b\mathbf{k}$. This calculation is performed at each of L^3 elementary cells $\Omega_{\mathbf{k}} \subset \Omega_L$, which presupposes substantial numerical costs in the limit of large L.

Figure 3.1 shows the example of a computational box with a 3D lattice-type molecular structure of $4 \times 4 \times 2$ atoms and the calculated lattice sum of electrostatic potentials. Note that in our approach we have the opportunity to verify the results of tensor calculation using subroutines from the tensor-structured Hartree-Fock solver [24].

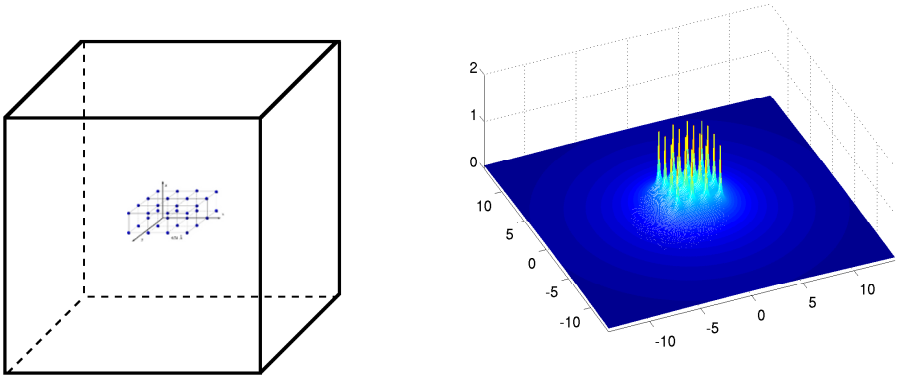

Figure 3.1: Example of $4 \times 4 \times 2$ lattice compound in a computational box and calculated potential sum.

In case (B), the 3D summation over L^3 cells in the limit of large L is considered as the hard computational task arising in the numerical treatment of extended systems in a supercell. The commonly used methods, know in the literature as the Ewald summation algorithms

[13], are based on a certain specific local-global decomposition of the Newton kernel (see [44, 20, 8])

$$\frac{1}{r} = \frac{\tau(r)}{r} + \frac{1-\tau(r)}{r},$$

where the traditional choice of the cutoff function τ is the complementary error function

$$\tau(r) = \mathrm{erfc}(r) := \frac{2}{\sqrt{\pi}} \int_r^\infty \exp(-t^2) dt.$$

In this paper, we introduce the new approach to this summation problem using the grid-based low-rank tensor approximation and fast tensor arithmetics, applied to the simultaneous summation of the projected core potentials in (3.1) over the supercell. The proposed tensor approach is not limited to the special case of the Newton kernel $\frac{1}{\|x\|}$, and it can be applied to the general class of shift-invariant well separable generating potentials.

Let Ω_{N_L} be the $N_L \times N_L \times N_L$ uniform grid on Ω_L with the same mesh-size h as above, and introduce the corresponding space of piecewise constant basis functions of the dimension N_L^3. In this construction we have

$$N_L = n + n(L-1) = Ln. \tag{3.2}$$

Similar to (2.10), we introduce the rank-R "master" tensor defined on the auxiliary box $\widetilde{\Omega}_L$ by scaling Ω_L with factor 2.

$$\widetilde{\mathbf{P}}_{L,R} = \sum_{q=1}^{R} P_q^{(1)} \otimes P_q^{(2)} \otimes P_q^{(3)} \in \mathbb{R}^{2N_L \times 2N_L \times 2N_L},$$

and let $\mathcal{W}_{\nu(k_i)}$, $i = 1, 2, 3$, be the directional windowing operators associated with the lattice vector $\mathbf{k}$.

Theorem 3.1 *The projected tensor of the interaction potential $v_{c_L}(x)$, $x \in \Omega_L$, representing the full lattice sum over M_0 charges can be presented by the canonical tensor $\mathbf{P}_{c_L}$ with the rank $R_0 \le M_0 R$,*

$$\mathbf{P}_{c_L} = \sum_{\nu=1}^{M_0} Z_\nu \sum_{q=1}^{R} \Big(\sum_{k_1=0}^{L-1} \mathcal{W}_{\nu(k_1)} P_q^{(1)}\Big) \otimes \Big(\sum_{k_2=0}^{L-1} \mathcal{W}_{\nu(k_2)} P_q^{(2)}\Big) \otimes \Big(\sum_{k_3=0}^{L-1} \mathcal{W}_{\nu(k_3)} P_q^{(3)}\Big). \tag{3.3}$$

The numerical cost and storage size are bounded by $O(M_0 R L N_L)$, and $O(M_0 R N_L)$, respectively.

Proof. For the moment, we fix index $\nu = 1$ in (3.1) and consider only the second sum defined on the complete domain Ω_L,

$$\widehat{v}_{c_L}(x) = \sum_{k_1,k_2,k_3=0}^{L-1} \frac{Z_\nu}{\|x - a_\nu(k_1,k_2,k_3)\|}, \quad x \in \Omega_L. \tag{3.4}$$

Then the projected tensor representation of $\widehat{v}_{c_L}(x)$ takes the form

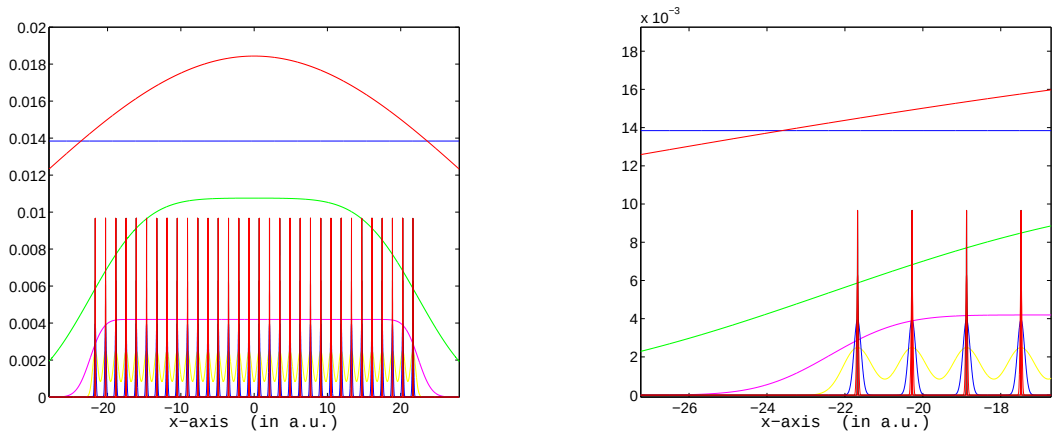

Figure 3.2: Left: agglomerated canonical vectors for a sum of Newton kernels for a cluster $32 \times 1 \times 1$ atoms in a box. Right: zoomed potential from the left.

$$\widehat{\mathbf{P}}_{c_L} = Z_\nu \sum_{k_1,k_2,k_3=0}^{L-1} \mathcal{W}_{\nu(\mathbf{k})} \widetilde{\mathbf{P}}_{L,R} = Z_\nu \sum_{k_1,k_2,k_3=0}^{L-1} \sum_{q=1}^{R} \mathcal{W}_{\nu(\mathbf{k})} (P_q^{(1)} \otimes P_q^{(2)} \otimes P_q^{(3)}) \in \mathbb{R}^{N_L \times N_L \times N_L},$$

where the 3D shift vector is defined by $\nu(\mathbf{k}) = \mathbf{k} - \mathbf{1}$ with $\mathbf{k} \in \mathbb{Z}^{L \times L \times L}$. Taking into account the separable representation of the Ω_L-windowing operator (tracing onto $N_L \times N_L \times N_L$ window),

$$\mathcal{W}_{\nu(\mathbf{k})} = \mathcal{W}^{(1)}_{\nu(k_1)} \otimes \mathcal{W}^{(2)}_{\nu(k_2)} \otimes \mathcal{W}^{(3)}_{\nu(k_3)},$$

we reduce the above summation to (omitting factor Z_ν)

$$\widehat{\mathbf{P}}_{c_L} = \sum_{q=1}^{R} \sum_{k_1,k_2,k_3=0}^{L-1} \mathcal{W}_{\nu(k_1)} P_q^{(1)} \otimes \mathcal{W}_{\nu(k_2)} P_q^{(2)} \otimes \mathcal{W}_{\nu(k_3)} P_q^{(3)}.$$

Using standard multilinear algebra on canonical tensors, the latter 3D-sum can be simplified to a rank-R tensor obtained by one-dimensional summations,

$$\begin{aligned}
\widehat{\mathbf{P}}_{c_L} &= \sum_{q=1}^{R} (\sum_{k_1=0}^{L-1} \mathcal{W}_{\nu(k_1)} P_q^{(1)}) \otimes (\sum_{k_2,k_3=0}^{L-1} \mathcal{W}_{\nu(k_2)} P_q^{(2)} \otimes \mathcal{W}_{\nu(k_3)} P_q^{(3)}) \\
&= \sum_{q=1}^{R} (\sum_{k_1=0}^{L-1} \mathcal{W}_{\nu(k_1)} P_q^{(1)}) \otimes (\sum_{k_2=0}^{L-1} \mathcal{W}_{\nu(k_2)} P_q^{(2)}) \otimes (\sum_{k_3=0}^{L-1} \mathcal{W}_{\nu(k_3)} P_q^{(3)}).
\end{aligned}$$

Weighted summation over M_0 charges leads to the desired representation. The numerical cost can be estimated by taking into account the standard properties of canonical tensors. ■

Figures 3.2 illustrate the shape of canonical vectors in the $L \times 1 \times 1$ lattice sum for $L = 32$, and its zoom at the left part of the box. Here $R = 25$ and $n = 4096$, $\varepsilon = 10^{-6}$. This figure demonstrates how the tensor summation incorporates simultaneously the local and global components in the decomposition of basic Newton potential thus reproducing several localization scales upon the given accuracy $\varepsilon > 0$ (cf. with Ewald summation techniques [13]

based on the two-level separation). The canonical vectors of the lattice sum in each spatial variable do not depend on other variables. For example, shapes of the canonical vectors in the first variable for $L \times L \times L$ lattice sum with $L = 32$ will be the same as in Figure 3.2.

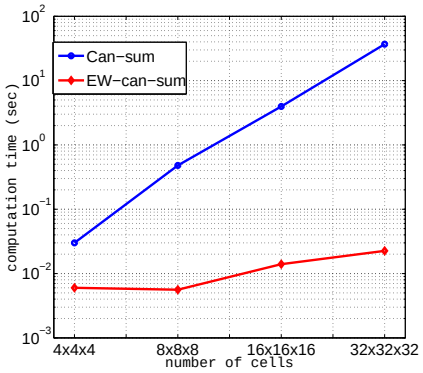

Figure 3.3: CPU times for calculating the total sum of nuclear potentials (in log scaling) for 3D $L \times L \times L$ lattice by using direct summation in canonical format (blue line) and tensor-type lattice summation (red line).

The constructive tensor representation (3.3) reduces dramatically the numerical costs and storage consumptions. Figure 3.3 illustrate the linear scaling in L for tensor summation method. Contrary to the direct canonical summation of the nuclear potentials on a 3D grid which scales linearly in the size of the cubic lattice, L^3, the directionally agglomerated canonical summation time scales linearly in L, i.e. practically remains constant.

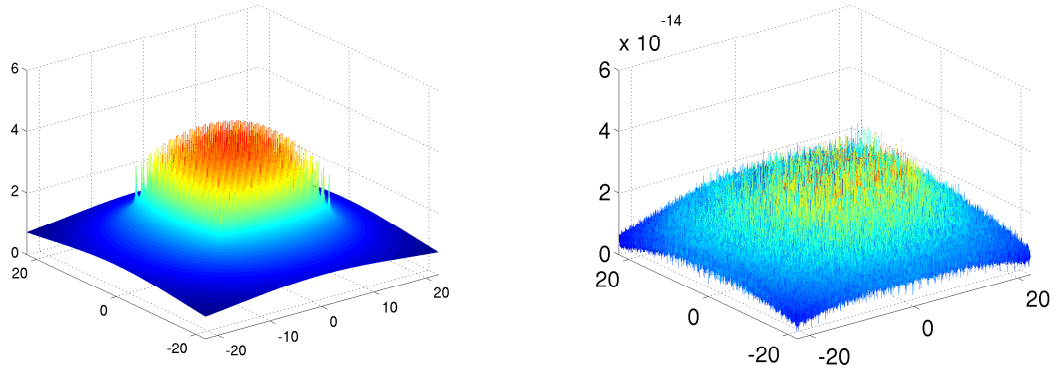

Figure 3.4: Left: the electrostatic potential of the cluster of $32 \times 32 \times 2$ Hydrogen atoms in a box. Right: the absolute error of the agglomerated canonical sum on this cluster by (3.3).

To illustrate the accuracy of the tensor-structured calculations, we use the subroutines from our black-box Hartree-Fock solver implemented in Matlab. In particular, we compare numerically the tensor sum obtained by the agglomerated canonical vectors and the same configuration calculated by a routine in our solver for computing the nuclear potential in the core Hamiltonian [24]. Figure 3.4 shows that the error of the tensor based summation using

agglomerated canonical vectors for a cluster of $32 \times 32 \times 2$ cells (a cluster of 1024 Hydrogen atoms) is close to machine accuracy $\sim 10^{-14}$.

In the limit of large L the lattice sum $\mathbf{P}_L$ of the Newton kernels converges only conditionally. The same is true in the periodic setting. In particular, the maximum norm increases as $C_1 \log L$, $C_2 L$ and $C_3 L^2$ for 1D, 2D and 3D sums, respectively. This issue is of special significance in the periodic setting, dealing with the infinite sums.

Figure 3.5 presents the value of the potential sum p_0 at the center of the supercell vs. L for $L \times 1 \times 1$, $L \times L \times 1$ and $L \times L \times L$ lattice sums for $L = 2, 4, 8, ..., 128$. The expected asymptotic behaviour in L is easily seen.

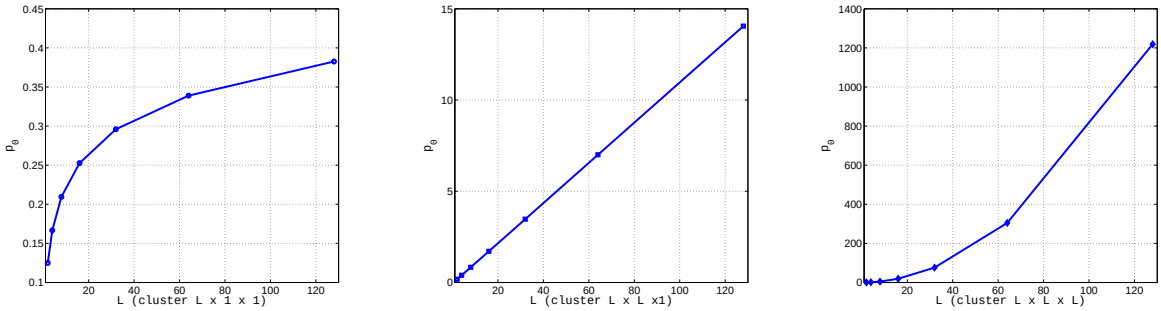

Figure 3.5: Potential sum p_0 at the center of the supercell vs. L for $L \times 1 \times 1$, $L \times L \times 1$ and $L \times L \times L$ lattice sums.

In the traditional Ewald-type summation techniques the regularization of lattice sums is implemented by subtraction of the analytically precomputed constants describing the asymptotic behavoiur in L. In our tensor summation method this problem is solved by algebraic approach by using the Richardson extrapolation techniques applied on a sequence of supercells with increasing size L, $2L$, $4L$, etc. Denoting the target value of the potential by p_L, the extrapolation formulas for the linear and quadratic behaviour take form

$$2p_L - p_{2L}, \quad \text{and} \quad (4p_L - p_{2L})/3,$$

respectively. Figure 3.6 indicates that the potential sum computed at the same point as for the previous example (in the case of $L \times L \times 1$ and $L \times L \times L$ lattices) converges to the limiting values after application of the Richardson extrapolation.

Table 3.1 illustrate the complexity scaling $O(N_L L)$ for the tensor lattice summation in supercells of size L for $L \times L \times 1$ and $L \times L \times L$. We observe the L^2 scaling which confirms our theoretical estimates.

L	2	4	8	16	32	64	128
$L \times L \times 1$	0.003	0.0041	0.0073	0.025	0.128	0.65	2.96
$L \times L \times L$	0.003	0.005	0.0098	0.039	0.19	0.88	4.01

Table 3.1: Times (in sec) vs. L for lattice summation of the tensor $\mathbf{P}_{c_L}$ on the clusters $L \times L \times 1$ and $L \times L \times L$.

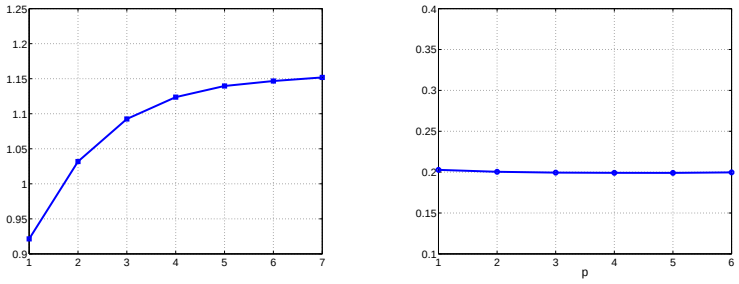

Figure 3.6: Regularized potential sum $\widehat{p}_0$ vs. m with $L = 2^m$, for $L\times L\times 1$ (left) and $L\times L\times L$ (red) lattice sums.

3.2 Tensor sum of the electrostatic potentials in a periodic setting

In the periodic case, further called case (P), we introduce the periodic cell $\mathcal{R} = b\mathbb{Z}^d$, $d = 1, 2, 3$, and consider a 3D T-periodic supercell of size $T \times T \times T$, with $T = bL$. The total electrostatic potential in Ω_L is obtained by the respective summation over the supercell Ω_L for possibly large L. Then the electrostatic potential in any of T-periods is obtained by replication of the respective data from Ω_L. Recall that in the limit of large L the lattice sum $\mathbf{P}_L$ of the Newton kernels converges only conditionally. The maximum norm increases as $C_1 \log L$, $C_2 L$ and $C_3 L^2$ for 1D, 2D and 3D sums, respectively. To approach the limiting case $L \to \infty$ we compute a on $\mathbf{P}_L$ on a sequence of large parameters $L, 2L, 4L$ etc. and then apply the Richardson extrapolation as described in §3.1.

The potential sum $v_{c_L}(x)$ is designated at each elementary unit-cell in Ω_L by the same value (**k**-translation invariant). Consider the case $d = 3$. Supposing for simplicity that L is odd, $L = 2p+1$, the reference value of $v_{c_L}(x)$ will be computed at the central cell Ω_0, indexed by $(p+1, p+1, p+1)$, by summation over all the contributions from L^3 elementary sub-cells in Ω_L,

$$v_0(x) = \sum_{\nu=1}^{M_0} \sum_{k_1,k_2,k_3=1}^{L} \frac{Z_\nu}{\|x - a_\nu(k_1, k_2, k_3)\|}, \quad x \in \Omega_0. \tag{3.5}$$

In case (P), the projected tensor can be computed by using simple modification of the representation in case (E).

Lemma 3.2 *The projected tensor of v_{Ω_L} for the full sum over M_0 charges can be presented by rank-$(M_0 R)$ canonical tensor. The computational cost is estimated by $O(M_0 RnL)$, while the storage size is bounded by $O(M_0 Rn)$.*

Proof. We fix index $\nu = 1$ in (3.5) and chose the central cell Ω_0 as above to obtain

$$v_{\Omega_L}(x) = \sum_{k_1,k_2,k_3=1}^{L} \frac{Z_\nu}{\|x - a_\nu(k_1, k_2, k_3)\|}, \quad x \in \Omega_0, \tag{3.6}$$

for the local lattice sum on the index set $n \times n \times n$, and

$$\mathbf{P}_{\Omega_0} = Z_\nu \sum_{k_1,k_2,k_3=1}^{L} \mathcal{W}_{\nu(\mathbf{k})} \mathbf{P}_{\Omega_0} = Z_\nu \sum_{k_1,k_2,k_3=1}^{L} \sum_{q=1}^{R_\mathcal{N}} \mathcal{W}_{\nu(\mathbf{k})} P_q^{(1)} \otimes P_q^{(2)} \otimes P_q^{(3)} \in \mathbb{R}^{n\times n\times n},$$

for the corresponding local projected tensor of small size $n \times n \times n$. Here we adapt the Ω-windowing operator, $\mathcal{W}_{\nu(\mathbf{k})} = \mathcal{W}^{(1)}_{\nu(k_1)} \otimes \mathcal{W}^{(2)}_{\nu(k_2)} \otimes \mathcal{W}^{(3)}_{\nu(k_3)}$, that projects onto the small $n \times n \times n$ unit cell by shifting on the lattice vector $\mathbf{k} = (k_1, k_2, k_3)$. Now the canonical representation follows by the arguments as in the proof of Theorem 3.1. The complexity analysis is similar to case (E). ■

Figure 3.7 shows the agglomerated canonical vectors for a lattice structure in a periodic setting.

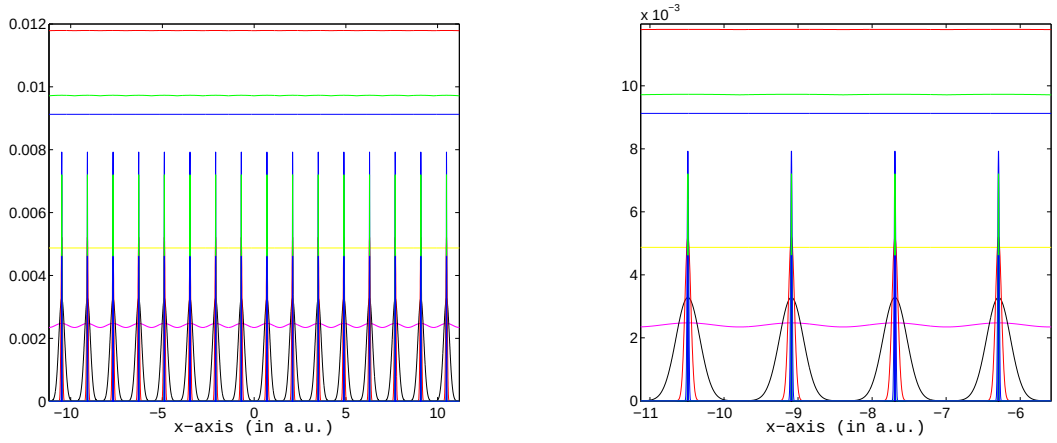

Figure 3.7: Periodic canonical vectors in the $L \times 1 \times 1$ lattice sum, $L = 16$ (left); Zooming of four periods (right).

The results of Rechardson extrapolation are illustrated in Figure 3.6.

Results in Sections 3.1 and 3.2 can be used in various applications, in particular, in Hartree-Fock calculations.

4 QTT ranks of the assembled canonical vectors in the lattice sum

Agglomerated canonical vectors in the rank-R tensor representation (3.3) are defined over large uniform grid of size N_L. Hence numerical cost for evaluation of each of these $3R$ vectors scales as $O(N_L L)$, which might become too expensive for large L (recall that $N_L = nL$ scales linear in L). Using quantics-TT (QTT) approximation [28], this cost can be reduced to the logarithmic scale in N_L, while the storage need will become $O(\log N_L)$ only.

Our QTT-rank estimates are based on three main ingredients: the global canonical tensor representation of $1/\|x\|$, $x \in \mathbb{R}^3$, on a supercell [18, 1], as in Proposition 2.1, QTT approximation to the Gaussian (Proposition 4.1) and the new result on the block QTT decomposition (Lemma 4.2 below).

The next statement presents the QTT-rank estimate for Gaussian vector obtained by uniform sampling of $\mathrm{e}^{-\frac{x^2}{2p^2}}$ on the finite interval [11].

Proposition 4.1 *Suppose uniform grid points $-a = x_0 < x_1 < \cdots < x_N = a$, $x_i = -a + hi$, $N = 2^L$ are given on an interval $[-a, a]$, and the vector $G = [g_i] \in \mathbb{R}^N$ is defined by its elements $g_i = \mathrm{e}^{-\frac{x_i^2}{2p^2}}$, $i = 0, ..., N-1$. For given $\varepsilon > 0$, assume that $\mathrm{e}^{-\frac{a^2}{2p^2}} \le \varepsilon$. Then there exists the QTT approximation G_r of the accuracy $||G - G_r||_\infty \le c\varepsilon$, with the ranks bounded by*

$$rank_{QTT}(G_r) \le c \log(\frac{p}{\varepsilon}),$$

where c does not depend on a, p, ε or N.

Proof. The result follows by a combination of Lemma 2 and Remark 3 in [11]. In fact, the condition $\mathrm{e}^{-\frac{a^2}{2p^2}} \le \varepsilon$ implies the relation

$$a \ge a_\varepsilon = \sqrt{2} p \log^{1/2}(1/\varepsilon). \tag{4.1}$$

Combining (4.1) and the rank-r truncated Fourier series representation G_r leads to the error bound

$$||G - G_r||_\infty \le c \left(1 + \frac{1}{p}\sqrt{\log \frac{p}{\varepsilon(1+a)}}\right) \varepsilon.$$

Hence, the result follows by substitution $\varepsilon \mapsto \frac{\varepsilon}{p}$. ∎

Next Lemma proves the important result that the QTT rank of a weighted sum of regularly shifted bumps (see Fig. 4.1) does not exceed the product of QTT ranks of the individual sample and the weighting factor.

Lemma 4.2 *Let $N = 2^L$ with the exponent $L = L_1 + L_2$, where $L_1, L_2 \ge 1$, and assume that the index set $I := \{1, 2, ..., N\}$ is split into $n_2 = 2^{L_2}$ equal non-overlapping subintervals $I = \cup_{k=1}^{n_2} I_k$, each of length $n_1 = 2^{L_1}$. Given n_1-vector X_0 that obeys the rank-r_0 QTT representation, define N-vectors X_k, $k = 1, ..., L_2$,*

$$X_k(i) = \begin{cases} X_0(:) & \text{for } i \in I_k \\ 0 & \text{for } i \in I \setminus I_k, \end{cases} \tag{4.2}$$

and denote $X = X_1 + ... + X_{L_2}$. Then for any choice of N-vector F, we have

$$rank_{QTT}(F \odot X) \le rank_{QTT}(F)\, r_0.$$

Proof. Since all vectors X_k ($k = 1, ..., L_2$) have non-intersecting supports, I_k, the L_2-level block quantics representation of X (see [28]) becomes separable and, we obtain the separable decomposition

$$\mathcal{Q}_L(X_1 + ... + X_{L_2}) = (\otimes_{k=1}^{L_2} \mathbf{1}) \otimes \mathcal{Q}_{L_1}(X_0), \quad \mathbf{1} = (1, 1)^T,$$

resulting in the rank bound

$$rank_{QTT}(X) \le r_0.$$

Combining this with the standard rank estimate for Hadamard product of tensors completes the proof. ∎

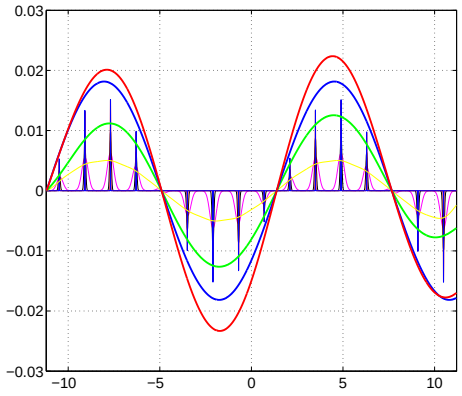

Figure 4.1: The agglomerated canonical vectors for the lattice sum modulated by a sin-function.

Remark 4.3 *Lemma 4.2 provides the constructive algorithm and rigorous proof of the low QTT-rank decomposition for certain class of Bloch functions [2] and Wannier-type functions.*

Figure 4.1 illustrates shapes of the agglomerated canonical vectors modulated by a sin function imitating the construction of the Wannier-type functions.

Now we are able to estimate QTT ranks of the agglomerated canonical vectors representing the lattice sum. In this study, we analyze the canonical decomposition based on the initial (non-optimized) quadrature (2.6) - (2.7) as in Proposition 2.1, where each term is obtained by sampling of a Gaussian on the uniform 3D grid. In practice, we apply the optimized quadrature obtained from the previous one by certain algebraic rank reduction [1]. This optimization procedure slightly modifies the shape of canonical vectors, however, the numerical tests indicate merely the same QTT ranks as predicted by our theory for the Gaussian-type vectors.

Lemma 4.4 *For given tolerance $\varepsilon > 0$, suppose that the set of Gaussian functions $S := \{g_k = e^{-t_k^2\|x\|^2}\}$, $k = 0, 1, ..., M$, representing canonical vectors in tensor decomposition $\mathbf{P}_R$, is specified by parameters in (2.5). Let us split the set S into two subsets $S = S_{loc} \cup S_{glob}$, such that*

$$S_{loc} := \{g_k : a_\varepsilon(g_k) \le b\} \quad \text{and} \quad S_{glob} = S \setminus S_{loc}.$$

where $a_\varepsilon(g_k)$ is defined by (4.1). Then the QTT-rank of each canonical vector v_q, $q = 1, ..., R$, in (3.3), where $R = M + 1$, corresponding to S_{loc} obeys the uniform in L rank bound

$$r_{QTT} \le C \log(1/\varepsilon).$$

For vectors in S_{glob} we have the rank estimate

$$r_{QTT} \le C \log(L/\varepsilon).$$

Proof. In our notation we have $1/(\sqrt{2}p_k) = t_k = (k \log M)/M$, $k = 1, ..., M$ ($k = 0$ is the trivial case). We omit the constant factor $\sqrt{2}$ to obtain $p_k = M/(k \log M)$.

For functions $g_k \in S_{loc}$, the relation (4.1) implies

$$O(1) = b \geq a_\varepsilon(g_k) = \sqrt{2} p_k \log^{1/2}(1/\varepsilon),$$

implying the uniform bound $p_k \leq C$, and then the rank estimate $r_{QTT} \leq C \log(1/\varepsilon)$ in view of Proposition 4.1. Now we apply Lemma 4.2 to obtain the uniform in L rank bound.

For globally supported functions in S_{glob} we have $bL \geq a_\varepsilon \simeq p_k \log^{1/2}(1/\varepsilon) \geq b$, hence we will consider all these function on the maximal support of the size of supercell, bL, and set $a = bL$. Using the trigonometric representation as in the proof of Lemma 2 in [11], we conclude that for each fixed k the shifted Gaussians, $g_{k,\ell}(x) = e^{-t_k^2 \|x - \ell b\|^2}$ $(\ell = 1, ..., L)$, can be approximated by shifted trigonometric series

$$G_r(x - b\ell) = \sum_{m=0}^{M} C_m p \mathrm{e}^{-\frac{\pi^2 m^2 p^2}{2a^2}} \cos\left(\frac{\pi m (x - b\ell)}{a}\right), \quad a = bL,$$

which all have the common trigonometric basis containing about $rank_{QTT}(G_r) = O(\log(\frac{p_k}{\varepsilon})) = O(\log(\frac{bL}{\varepsilon}))$ terms. Hence the sum of shifted Gaussian vectors over L unit cells will be approximated with the same QTT-rank bound as each individual term in this sum, which proves the assertion. ■

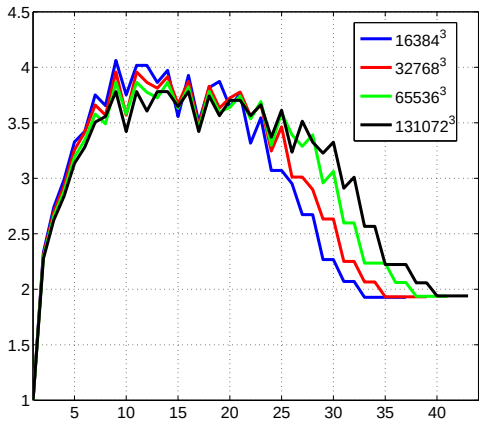

Figure 4.2: QTT-ranks of the canonical vectors of a single 3D Newton kernel discretized on a cubic grids of size $n^3 = 16384^3$, 32768^3, 65536^3 and 131072^3.

Based on the previous statements, we arrive at the following result.

Theorem 4.5 *The projected tensor of v_{c_L} for the full sum over a single charge can be presented by the rank-R QTT-canonical tensor*

$$\mathbf{P}_{c_L} = \sum_{q=1}^{R} (\mathcal{Q} \sum_{k_1=1}^{L} \mathcal{W}_{\nu(k_1)} P_q^{(1)}) \otimes (\mathcal{Q} \sum_{k_2=1}^{L} \mathcal{W}_{\nu(k_2)} P_q^{(2)}) \otimes (\mathcal{Q} \sum_{k_3=1}^{L} \mathcal{W}_{\nu(k_3)} P_q^{(3)}), \qquad (4.3)$$

where the QTT-rank of each canonical vector is bounded by $r_{QTT} \leq C \log(L/\varepsilon)$. The computational cost is estimated by $O(RLr_{QTT}^3)$, while the storage size scales as $O(R \log^2(L/\varepsilon))$.

Figure 4.2 represents QTT-ranks of the canonical vectors of a single 3D Newton kernel discretized on a large cubic grids.

Figure 4.3 demonstrates that the average QTT ranks of the agglomerated canonical vectors for $k = 1, ..., R$, scale logarithmically both in L and in the total grid-size $n = N_L$.

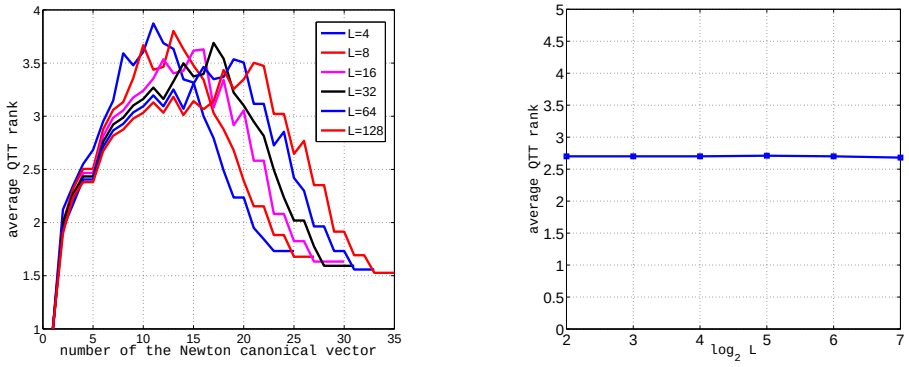

Figure 4.3: Left: QTT ranks of the agglomerated canonical vectors vs. L for fixed grid size $n^3 = 16384^3$. Right: Average QTT-ranks over R canonical vectors vs. $\log L$ for 3D evaluation of the $L \times 1 \times 1$ chain of Hydrogen atoms on $n \times n \times n$ grids, $n = 2048$, 4096, 8192, 16384.

5 Conclusions

We introduce the rank-adaptive tensor method for fast and accurate calculation of $L \times L \times L$ lattice sums of Coulomb interactions on large 3D periodic-structured compounds discretized on $N \times N \times N$ 3D Cartesian grids. The two practically interesting cases have been considered: supercell in a box and supercell in periodic setting.

For the case of 3D supercell in a box, our approach exhibits the linear scaling in L for both computational work and storage size. In the periodic setting, the storage size is uniformly bounded in L. For example, one can easily handle a lattice of the size of 128^3 units cells ($L = 128$) using Matlab at a SUN-station of the 8 AMD Opteron cluster (see Table 3.1). In our computations the grid size for 3D grid-based numerical simulation can be as large as 131072^3 at moderate times, providing the mesh size of the order of 10^{-4} a.u. in electronic structure calculations. Comparison of the direct canonical sums of the electrostatic potentials computed within our tensor-structured Hartree-Fock solver and the agglomerated tensor summation demonstrates the accuracy at the level of machine precision, 10^{-14}.

For both models, we prove that QTT approximation method reduces the complexity to logarithmic scaling in the total grid size, $O(\log N)$. This suggests the efficient approach to numerical simulations on large $L \times L \times L$ lattices. In this case a combination with the fast multipole method [16] and FFT seems promising.

It is worth to note that the sum of electrostatic potentials is calculated in a whole computational box in a convenient structured form, which is suitable for further numerical treatment of the involved 3D quantities by tensor methods in 1D complexity, including integration, differentiation, and other algebraic transforms.

Our approach can be also applied to a wide class of commonly used chemical potentials, in particular, to Coulomb-type, Yukawa, Helmholtz, Slater, Stokeslet, Lennard-Jones or van der Waals interactions. In all these cases the low-rank tensor decomposition can be proved to exist and can be constructed by the analytic-algebraic methods as in the case of Newton kernel.

6 Appendix: Short introduction to tensor formats

Separable representation of the multidimensional arrays in the Tucker and canonical tensor formats, were since long known in the computer science community [35], where they were mostly used in processing of the multidimensional experimental data in chemometrics, psychometrics and in signal processing. The remarkable approximating properties of the Tucker and canonical decomposition for wide classes of function related tensors were revealed in [26, 31], promoting its usage as a tool for the numerical treatment of the multidimensional problems in numerical analysis.

A tensor is a multidimensional array given by a d-tuple index set,

$$\mathbf{A} = [a_{i_1,\ldots,i_d}] \in \mathbb{R}^{n_1\times\ldots\times n_d} \quad i_\ell \in \{1,\ldots,n_\ell\}.$$

It is an element of a linear vector space equipped with the Euclidean scalar product. For tensor with equal sizes $n_\ell = n$, $\ell = 1,\ldots d$, the required storage is $n^{\otimes d}$. To get rid of the exponential growth of the tensor with the dimension d, the rank-structured representations of the multidimensional arrays can be employed. We use as a building block a rank-1 tensor, which is a tensor product of vectors in each dimension,

$$\mathbf{A} = u^{(1)} \otimes \ldots \otimes u^{(d)} \in \mathbb{R}^{n_1\times\ldots\times n_d}$$

with entries $u_{i_1,\ldots i_d} = u^{(1)}_{i_1} \cdots u^{(d)}_{i_d}$. Taking a sum of R rank-1 tensors with some weights c_k one comes to the canonical rank-R representation,

$$\mathbf{A} = \sum_{k=1}^{R} c_k u^{(1)}_k \otimes \ldots \otimes u^{(d)}_k, \quad c_k \in \mathbb{R}, \tag{6.1}$$

where $u^{(\ell)}_k$ are normalized vectors.

The Tucker decomposition is constructed using the orthogonal projection of the original tensor by the orthogonal matrices. It is also a sum of the tensor products,

$$\mathbf{A} = \sum\nolimits_{\nu_1=1}^{r_1} \ldots \sum\nolimits_{\nu_d=1}^{r_d} \beta_{\nu_1,\ldots,\nu_d}\, v^{(1)}_{\nu_1} \otimes \ldots \otimes v^{(d)}_{\nu_d}, \quad \ell = 1,\ldots,d,$$

where $\mathbf{r} = (r_1,\ldots,r_d)$ is the Tucker rank, $\boldsymbol{\beta} = [\beta_{\nu_1,\ldots,\nu_d}]$ is the core tensor, and the set of orthonormal vectors $v^{(\ell)}_{\nu_\ell} \in \mathbb{R}^{n_\ell}$, form the orthogonal matrices of the Tucker projection.

The rank-structured tensor representation provides 1D complexity of multilinear operations with multidimensional tensors. In particular, it was shown in [32, 23], that tensor-structured calculation of the $3D$ convolution integrals can be reduced to a sequence of 1D convolution transforms, and 1D Hadamard and scalar products.

In the QTT approximation we also apply the so-called tensor train (TT) format [41], which is the particular case of the matrix-product states (MPS) decomposition, introduced in quantum chemistry and quantum information theory [48, 45]. Any entry of a dth order tensor in this format is given by

$$a(i_1, i_2, \ldots, i_d) = A^{(1)}_{i_1} A^{(2)}_{i_2} \ldots A^{(d)}_{i_d}, \tag{6.2}$$

where each $A^{(k)}_{i_k} = A^{(k)}(\alpha_{k-1}, i_k, \alpha_k)$ is $r_{k-1} \times r_k$ matrix depending on i_k with the convention $r_0 = r_d = 1$. Storage size for $n^{\otimes d}$ TT tensor is bounded by $O(dr^2 n)$, $r = \max r_k$. The algebraic operations on TT tensors can be implemented with linear complexity scaling in n and d.

In 2009 the quantics TT (QTT) tensor approximation method was introduced[2] and rigorously proved to provide logarithmic scaling in storage for a wide class of function generated vectors and multidimensional tensors, see also [28]. In particular, the QTT representation of function-related vectors of size $N = q^L$, $(q = 2, 3, ...)$ needs only

$$q \cdot L \cdot r^2 \ll q^L$$

numbers to store, where r is the QTT-rank of $q \times q \times ... \times q$ tensor of order L, reshaped from the initial vector by q-adic folding [28]. For example, the N-vector $X = [x_i]$ is reshaped to its quantics image in $\mathbb{Q}_L := \bigotimes_{\ell=1}^{L} \mathbb{R}^q$ via q-coding,

$$i - 1 = \sum_{\ell=1}^{L} (j_\ell - 1) q^{\ell-1}, \quad j_\ell \in \{1, 2, ..., q\}.$$

Though the optimal choice is shown to be $q = 2$ or $q = 3$, the numerical implementations are usually performed with $q = 2$ (binary coding).

In [28] it was proven that the rank parameter r in the QTT approximation is a small constant for a wide class of functions discretized on the uniform grid. For example, $r = 1$ for complex exponents, and $r = 2$ for trigonometric functions and for Chebyshev polynomials (sampled on Chebyshev-Gauss-Lobatto grid). Moreover, $r \leq m + 1$ for polynomials of degree m, and r is a small constant for some wavelet basis functions, etc.

The numerical experiments on TT representation for some reshaped $N \times N$ matrices were presented in [42]. The QTT approximation method was proven to provide the low QTT-rank representation on a class of matrices associated with elliptic operators [21]. It also enables the multidimensional FFT [10], convolution [22] and wavelet [34] transforms all with logarithmic complexity scaling, $O(\log N)$.

References

[1] C. Bertoglio, and B.N. Khoromskij. *Low-rank quadrature-based tensor approximation of the Galerkin projected Newton/Yukawa kernels.* Comp. Phys. Communications, 183(4) (2012) 904–912.

[2] B.N. Khoromskij. *$O(d \log N)$-Quantics Approximation of N-d Tensors in High-Dimensional Numerical Modeling.* Preprint 55/2009, Max-Planck Institute for Mathematics in the Sciences, Leipzig 2009; http://www.mis.mpg.de/publications/preprints/2009/prepr2009-55.html.

[2] Bloch, André, "Les thormes de M.Valiron sur les fonctions entires et la thorie de l'uniformisation". Annales de la facult des sciences de l'Universit de Toulouse 17 (3): 1-22 (1925). ISSN 0240-2963.

[3] Boys, S. F., Cook, G. B., Reeves, C. M. and Shavitt, I. (1956). *Automatic Fundamental Calculations of Molecular Structure*. Nature, 178: 1207-1209.

[4] D. Braess. *Nonlinear approximation theory.* Springer-Verlag, Berlin, 1986.

[5] D. Braess. *Asymptotics for the Approximation of Wave Functions by Exponential-Sums.* J. Approx. Theory, 83: 93-103, (1995).

[6] E. Cancés, V. Ehrlacher, and Y. Maday. *Periodic Schrödinger operator with local defects and spectral pollution.* SIAM J. Numer. Anal. v. 50, No. 6, pp. 3016-3035.

[7] T. Darten, D. York and L. Pedersen. *Particle mesh Ewald: An $O(N \log N)$ method for Ewald sums in large systems.* J. Chem. Phys., 98, 10089-10091, 1993.

[8] M. Deserno and C. Holm. *How to mesh up Ewald sums. I. A theoretical and numerical comparison of various particle mesh routines.* J. Chem. Phys., 109(18): 7678-7693, 1998.

[9] M. Deserno and C. Holm. *How to mesh up Ewald sums. II. An accurate error estimate for the Particle-Particle-Particle-Mesh algorithm.* J. Chem. Phys. 109(7694), 1998.

[10] S.V. Dolgov, B.N. Khoromskij, and D. Savostyanov. *Superfast Fourier transform using QTT approximation.* J. Fourier Anal. Appl., 2012, vol.18, 5, 915-953.

[11] S.V. Dolgov, B.N. Khoromskij, and I. Oseledets. *Fast solution of multi-dimensional parabolic problems in the TT/QTT formats with initial application to the Fokker-Planck equation.* SIAM J. Sci. Comput., **34**(6), 2012, A3016-A3038.

[12] R. Dovesi, R. Orlando, C. Roetti, C. Pisani, and V.R. Sauders. *The Periodic Hartree-Fock Method and its Implementation in the CRYSTAL Code.* Phys. Stat. Sol. (b) **217**, 63 (2000).

[13] Ewald P.P. *Die Berechnung optische und elektrostatischer Gitterpotentiale.* Ann. Phys **64**, 253 (1921).

[14] I.P. Gavrilyuk, W. Hackbusch and B.N. Khoromskij. *Hierarchical Tensor-Product Approximation to the Inverse and Related Operators in High-Dimensional Elliptic Problems.* Computing 74 (2005), 131-157.

[15] L. Grasedyck, D. Kressner and C. Tobler. *A literature survey of low-rank tensor approximation techniques.* arXiv:1302.7121v1, 2013.

[16] L. Greengard and V. Rochlin. *A fast algorithm for particle simulations.* J. Comp. Phys. 73 (1987) 325.

[17] W. Hackbusch. *Tensor spaces and numerical tensor calculus.* Springer, 2012.

[18] W. Hackbusch and B.N. Khoromskij. *Low-rank Kronecker product approximation to multi-dimensional nonlocal operators. Part I. Separable approximation of multi-variate functions.* Computing **76** (2006), 177-202.

[19] T. Helgaker, P. Jørgensen, and J. Olsen. *Molecular Electronic-Structure Theory.* Wiley, New York, 1999.

[20] Philippe H. Hünenberger. *Lattice-sum methods for computing electrostatic interactions in molecular simulations.* CP492, L.R. Pratt and G. Hummer, eds., 1999, American Institute of Physics, 1-56396-906-8/99.

[21] V. Kazeev, and B.N. Khoromskij. *Explicit low-rank QTT representation of Laplace operator and its inverse.* SIAM Journal on Matrix Anal. and Appl., 33(3), 2012, 742-758.

[22] V. Kazeev, B.N. Khoromskij, and E.E. Tyrtyshnikov. *Multilevel Toeplitz matrices generated by tensor-structured vectors and convolution with logarithmic complexity.* SIAM J. Sci. Comput. 35-3 (2013), pp. A1511-A1536.

[23] V. Khoromskaia. *Numerical Solution of the Hartree-Fock Equation by Multilevel Tensor-structured methods.* PhD thesis, TU Berlin, 2010.

[24] V. Khoromskaia. *Black-box Hartree-Fock solver by tensor numerical methods.* Comp. Meth. in Applied Math., 2013 (to appear), doi: 10.1515/cmam-2013-0023. Preprint 90/2013, MPI MIS, Leipzig 2013.

[25] V. Khoromskaia, B.N. Khoromskij, and R. Schneider. *Tensor-structured calculation of two-electron integrals in a general basis.* SIAM J. Sci. Comput., **35**(2), 2013, A987-A1010.

[26] B.N. Khoromskij, *Structured Rank-$(r_1, ..., r_d)$ Decomposition of Function-related Tensors in $\mathbb{R}^d$.* Comp. Meth. in Applied Math., **6** (2006), 2, 194-220.

[27] B.N. Khoromskij. *Fast and Accurate Tensor Approximation of a Multivariate Convolution with Linear Scaling in Dimension.* J. Comp. Appl. Math. 234 (2010) 3122-3139.

[28] B.N. Khoromskij. *$O(d \log N)$-Quantics Approximation of N-d Tensors in High-Dimensional Numerical Modeling.* Constructive Approx. **34** (2011) 257–280. (Preprint 55/2009 MPI MiS, Leipzig 2009.)

[29] B.N. Khoromskij. *Introduction to Tensor Numerical Methods in Scientific Computing.* Lecture Notes, Preprint 06-2011, University of Zuerich, Institute of Mathematics, 2011, pp 1 - 238. http://www.math.uzh.ch/fileadmin/math/preprints/06_11.pdf

[30] B.N. Khoromskij. *Tensors-structured Numerical Methods in Scientific Computing: Survey on Recent Advances.* Chemometr. Intell. Lab. Syst. 110 (2012), 1-19.

[31] B. N. Khoromskij and V. Khoromskaia. *Low Rank Tucker Tensor Approximation to the Classical Potentials.* Central European J. of Math., **5**(3) 2007, 1-28.

[32] B.N. Khoromskij and V. Khoromskaia. *Multigrid tensor approximation of function related multidimensional arrays.* SIAM J. Sci. Comp. 31(4) (2009) 3002-3026.

[33] B.N. Khoromskij, V. Khoromskaia, and H.-J. Flad. *Numerical Solution of the Hartree-Fock Equation in Multilevel Tensor-structured Format.* SIAM J. Sci. Comp. 33(1) (2011) 45-65.

[34] Boris N. Khoromskij, and Sentao Miao. *Superfast Wavelet Transform Using QTT Approximation. I: Haar Wavelets.* Preprint 103/2013, MPI MiS, Leipzig 2013, submitted.

[35] T.G. Kolda and B.W. Bader. *Tensor Decompositions and Applications.* SIAM Rev. 51(3) (2009) 455–500.

[36] K.N. Kudin, and G.E. Scuseria, *Revisiting infinite lattice sums with the periodic Fast Multipole Method*, J. Chem. Phys. 121, 2886-2890 (2004).

[37] M. Lorenz, L. Maschio, M. Schütz, and D. Usvyat, *Local ab initio methods for calculating optical band gaps in periodic systems: II. Periodic density fitted local configuration interaction singles method for solids*, J. Chem. Phys., 137, 204119 (2012).

[38] S. A. Losilla, D. Sundholm, J. Juselius. *The direct approach to gravitation and electrostatics method for periodic systems.* J. Chem. Phys. 132 (2) (2010) 024102.

[39] D. Lindbo and A.-K. Tornberg. *Fast and spectrally accurate Ewald summation for 2-periodic electrostatic systems.* J. Chem. Phys. 136:164111, 2012, doi: 10.1063/1.4704177.

[40] M. Lorenz, D. Usvyat, and M. Schütz. *Local ab initio methods for calculating optical band gaps in periodic systems. I. Periodic density fitted local configuration interaction singles method for polymers.* J. Chem. Phys. **134**, 094101 (2011); doi: 10.1063/1.3554209.

[41] I.V. Oseledets, and E.E. Tyrtyshnikov. *Breaking the Curse of Dimensionality, or How to Use SVD in Many Dimensions.* SIAM J. Sci. Comp., 31 (2009), 3744-3759.

[42] I.V. Oseledets, *Approximation of $2^d \times 2^d$ matrices using tensor decomposition.* SIAM J. Matrix Anal. Appl., 31(4):2130-2145, 2010.

[43] C. Pisani, M. Schütz, S. Casassa, D. Usvyat, L. Maschio, M. Lorenz, and A. Erba. *CRYSCOR: a program for the post-Hartree-Fock treatment of periodic systems*, Phys. Chem. Chem. Phys., 2012, **14**, 7615-7628.

[44] A. Y. Toukmaji, and J. Board Jr. *Ewald summation techniques in perspective: a survey.* Computer Phys. Communication **95** (1996), 73-92.

[45] F. Verstraete, D. Porras, and J.I. Cirac. *DMRG and periodic boundary conditions: A quantum information perspective.* Phys. Rev. Lett., 93(22): 227205, Nov. 2004.

[46] Elena Voloshina, Denis Usvyat, Martin Schütz, Yuriy Dedkov and Beate Paulus. *On the physisorption of water on graphene: a CCSD(T) study.* Phys. Chem. Chem. Phys., 2011, 13, 12041-12047.

[47] O.V. Yazyev, E.N. Brothers, K.N. Kudin, and G.E. Scuseria, *A finite temperature linear tetrahedron method for electronic structure calculations of periodic systems*, J. Chem. Phys. 121, 2466-2470 (2004).

[48] S.R. White. *Density-matrix algorithms for quantum renormalization groups.* Phys. Rev. B, v. 48(14), 1993, 10345-10356.